# Chapter 2.

# Heat Capacity and Thermal Conductivity

Wash Day
Robert Wittig

## Contents

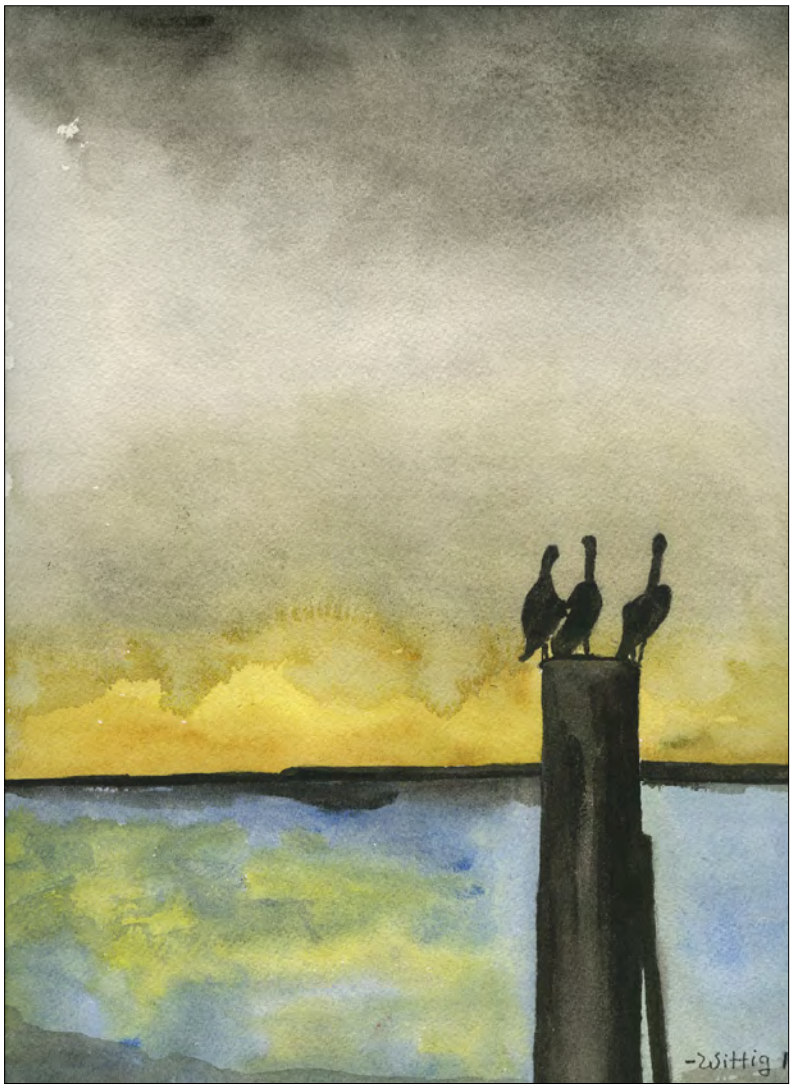


Birds of Lill
Robert Wittig

It is inexcusable for scientists to torture animals; let them make their experiments on journalists and politicians.

Henrik Ibsen

## 2.1. Preliminary Comments

To determine a system's thermodynamic properties, it is necessary to know how its stored (non-chemical) energy is distributed over the degrees of freedom of its particles and quasiparticles at a given temperature. In this chapter, we shall be concerned with the heat capacity and thermal conductivity of non-magnetic, electrically insulating crystals. In these systems, phonons are solely responsible for heat capacity and thermal conductivity, with the exception of very low temperatures (say ~ 1 K), where impurities, defects, and boundaries limit thermal conductivity.

Metals are different. Their ionic lattices give rise to phonons, including low frequency ones that result in good heat capacity. In fact, phonons play the dominant role in the heat capacity and thermal conductivity of metals at all but the lowest temperatures. Electrons play a significant role only at quite low temperatures. The reason electrons contribute so little is due to the fact that they are fermions. Therefore, only electrons that have energy near the Fermi level can move about freely and participate in heat capacity. The rest of the electrons are, so to speak, frozen out. The reason they are important at low temperatures is that the phonon contributions freeze out more rapidly than the electron contributions as temperature is lowered.

There is nothing so complicated that it cannot, with sufficient effort, be made more complicated.

To keep matters simple, the electronic contribution to the heat capacity and the thermal conductivity will not be considered. In other words, we shall deal with non-magnetic, electrical insulating crystals or, it can be said, the phonon contribution to the heat capacity of a metal.

In this chapter, we shall begin by using the distribution function for a canonical ensemble of bosons to obtain the average number of quanta in a given mode. Following this, elementary models of heat capacity and thermal conductivity will be introduced. More detailed models would require more time than we have available for these topics. It is hoped that the introductory treatment presented below will open the door to related topics, should you wish to pursue the subject further.

## 2.2. Canonical Ensemble of Bosons

The average number of quanta in a given mode is calculated here for a sample in thermal equilibrium at temperature $T$. This is done first for a 1D system, and the result is then extended to 3D. The 2D case is assigned as an exercise. The Boltzmann factor $e^{-E/k_BT}$ is used to obtain the average energy of the $k^{th}$ mode, which shall be denoted $\langle E_k \rangle$. It is not necessary to include the zero point energy unless chemical bonds are broken or phase transitions take place. These phenomena will not be considered here, so zero point energy

shall be suppressed. Also, in discussing heat capacity, it is assumed for the time being that all vibrations are harmonic. That is, anharmonicity is suppressed. However, you will see that anharmonicity proves to be crucial when it comes to thermal conductivity, and we will discuss its role there. It is also responsible for thermal expansion, phonon removal rates, and so on.

Because the energies available to the $k^{th}$ mode are integer multiples, $n_k$, of the energy quantum $\hbar\omega_k$, $\langle E_k \rangle$ is related trivially to the average number of quanta, $\langle n_k \rangle$:

$$\langle E_k \rangle = \hbar\omega_k \langle n_k \rangle = Z^{-1} \sum_{n=0}^{\infty} n\hbar\omega_k \exp\left(-\frac{n\hbar\omega_k}{k_B T}\right). \tag{2.1}$$

Explicit $\hbar$ will be used for a while; the Boltzmann constant is $k_B$; and the partition function, *Z*, is given by

$$Z = \sum_{n=0}^{\infty} \exp\left(-\frac{n\hbar\omega_k}{k_B T}\right). \tag{2.2}$$

Notational simplification is achieved by using $x = \exp(-\hbar\omega_k / k_B T)$, in which case eqn (2.1) gives

$$\langle n_k \rangle = Z^{-1} \sum_{n=0}^{\infty} n x^n = Z^{-1}\left(x + 2x^2 + 3x^3 ...\right). \tag{2.3}$$

Thus, eqn (2.2) becomes

$$Z = \sum_{n=0}^{\infty} x^n = 1 + x + x^2 ... = 1 + x(1 + x + x^2 ...) = 1 + xZ, \tag{2.4}$$

yielding a compact expression for the partition function:

$$Z = \frac{1}{1-x}. \tag{2.5}$$

The parenthetic term in eqn (2.3) can be written $x(1 + x + x^2 ...)^2$, which is identified as being equal to $xZ^2$. Thus, eqn (2.3) becomes

$$\langle n_k \rangle = xZ = \frac{x}{1-x}. \tag{2.6}$$

Finally, replacing *x* with $\exp(-\hbar\omega_k / k_B T)$ yields the standard form:

$$\langle n_k \rangle = \frac{1}{e^{\hbar\omega_k / k_B T} - 1}. \tag{2.7}$$

This is the average number of quanta excluding zero point for a thermal distribution of phonons whose energy quantum is $\hbar\omega_k$. It is the Bose-Einstein distribution for bosons at temperature *T*. The fact that an average value appears in eqn (2.7) does not mean that $\langle n_k \rangle$ is large. If $\langle n_k \rangle$ is small, the assumption of a canonical distribution gives a correct average value, but it turns out that $n_k$ fluctuates from one *k* value to the next. However, the mode density is usually large, in which case a smooth distribution of the number of modes versus energy can be recovered by averaging over some number of modes according to an *n*-point smoothing routine.

Referring to eqn (2.7), the corresponding expression for fermions differs in a way that is subtle and of enormous significance. The $-1$ is replaced by $+1$, and $\hbar\omega_k$ is replaced by $E - E_F$, where *E* is the energy of a single-particle state and $E_F$ is the Fermi energy. It is the energy of the highest occupied state at 0 K.[1]

$$f(E) = \frac{1}{e^{(E-E_F)/k_B T} + 1}. \tag{2.8}$$

The difference between eqns (2.7) and (2.8) is profound in the extreme. For example, the high temperature limit of eqn (2.7) is $k_B T/\hbar\omega_k$, whereas the high temperature limit of eqn (2.8) ( $k_B T >> E - E_F$ ) is ½. The low temperature limit of eqn (2.7) is $e^{-\hbar\omega_k / k_B T}$, whereas the low temperature limit of eqn (2.8) is 1 for $E - E_F < 0$, and 0 for $E - E_F > 0$. It is not possible for two or more identical fermions (electrons) to occupy a given single-particle state (spin-orbital), whereas phonons can occupy a given mode with as many quanta as possible, limited only by degeneracy and the Boltzmann factor. Figure 1 illustrates this difference.

We saw in Chapter 1 that the quantization of a field of harmonically coupled mass points yields phonons. These are massless bosons. There is no energy involved in their creation and annihilation other than the energy of their quanta. On the other hand, fermions have mass, so at the low energies of concern here we do not deal with their creation and annihilation. These processes take place at high energy because the field quanta (the fermions themselves) have mass whose energy is $mc^2$. In other words, the number of fermions is assumed to remain constant, obviating the need for a field theoretic description of their dynamics.

---

[1] Equation (2.8) is not correct, though it is an extremely accurate approximation for the systems and temperatures of concern. The term $E_F$ that appears in eqn (2.8) should be the chemical potential, $\mu$, which is also referred to as the Fermi *level*. Only at much higher temperatures than those of interest here does $\mu$ differ significantly from $E_F$. The Fermi energy is easier to visualize than the Fermi level. The latter is discussed in Chapter 3.

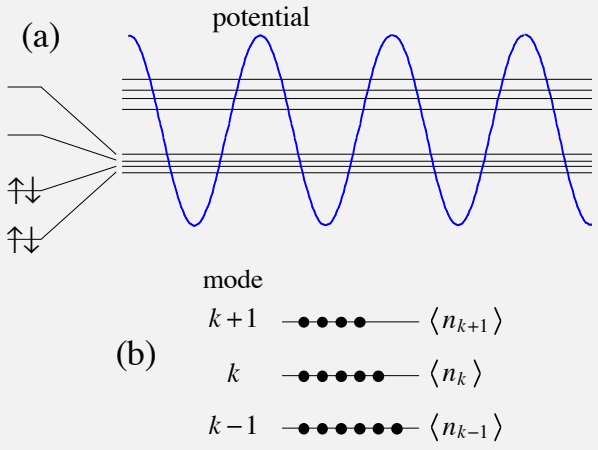


Figure 1. (a) Electrons in a 1D periodic potential occupy orbitals according to the Pauli exclusion principle: one per spin orbital. For a given temperature the distribution function is given by eqn (2.8). (b) A given phonon mode ($k$ value) has an energy quantum $\hbar\omega_k$. Many phonons (dots) can occupy the same mode. The average number of phonons per mode is given by eqn (2.7)

The bottom line is that fermions obey the Pauli exclusion principle, which sets their thermodynamic properties apart from those of bosons and other massless quasiparticles.

## 2.3. Heat Capacity

Despite the fact that the heat capacity of an electrically insulating crystal is conceptually straightforward, a first-principles calculation for a real crystal would be too arduous to be undertaken here. To strike a compromise, the underlying principles will be presented, and then a simple model due to Debye will be introduced and discussed. This model accounts for the main features of heat capacity, and it is applicable from the lowest to the highest temperatures. It is generally in reasonable agreement with experiment. This is not surprising given that the Debye model is an interpolation between the low and high temperature limits, each of which is on sound theoretical footing. These limiting cases are easy to derive and understand, and they will be discussed.

A good starting point is eqn (2.7). The heat capacity of a substance is the rate of change of its stored energy with temperature. In other words, if a 1 K temperature increase results in the stored energy of one mole of the substance increasing by Q Joules, the heat capacity $C$ is equal to $\mathrm{Q\ Joules \cdot K^{-1} \cdot mole^{-1}}$. For a crystal, there is little difference between the heat capacities at constant pressure and at constant volume, $C_P$ and $C_V$, respectively, because little work is done by thermal expansion of the crystal. Thus, we will drop the $P$ and $V$ subscripts and refer to the heat capacity simply as $C$. For a single mode (single $k$ value), the single-mode heat capacity $C_k$ is obtained straightaway by using eqns (2.1) and (2.7). The result is

$$C_k = \frac{\partial \langle E_k \rangle}{\partial T} = \hbar\omega_k \frac{\partial}{\partial T}\left(\frac{1}{e^{\Theta_k/T} - 1}\right), \tag{2.9}$$

where $\Theta_k = \hbar\omega_k / k_B$. Carrying out the differentiation yields

$$C_k = k_B \left( \frac{\Theta_k}{T} \right)^2 \frac{e^{\Theta_k / T}}{(e^{\Theta_k / T} - 1)^2} . \tag{2.10}$$

Notice that this result, which was easy to obtain, has nothing to do with the dimension of the space. It can be applied to 1D, 2D, and 3D models. The dimension of the space enters when we include the participating frequencies, which is done according to the dispersion relation. This is easy with 1D models, but it can prove challenging with 3D models. Again, we shall start with 1D and proceed to 3D.[2]

The *k*-space density, $\rho(k)$, is the number of modes per unit wave vector. Sometimes this is referred to as the density of states in *k*-space. This usage will be avoided, because we shall take the term "state" in the context of density of states to mean a fully resolved (non-degenerate) state that has a specified energy.

The *k*-space density $\rho(k)$ is now calculated and it is used to obtain the density of mode frequencies, $g(\omega)$. This is where the dispersion relation enters. The average energy is obtained by combining $g(\omega)$ with the average energy per mode. We shall start with $\rho_1(k)$ (the subscript denotes 1D) and the dispersion relation for one of the 1D models introduced earlier. The dispersion relation enables us to convert $\rho_1(k)$ to $g_1(\omega)$, the number of corresponding modes per unit frequency interval. In other words, $\rho_1(k)$ is mapped onto $g_1(\omega)$ using the relationship between *k* and $\omega$ given by the dispersion relation. Hereafter, the convention $\hbar = 1$ will be used unless otherwise noted.

## 2.4. One-Dimensional Monatomic Lattice

The *k*-space density for a 1D monatomic lattice, $\rho_1(k)$, is equal to $L/2\pi$, as indicated in Fig. 2. The dispersion relation that will be used in the material that follows is $\omega^2 = 4\Omega^2 \sin^2(ka/2)$. For positive frequencies, this dispersion relation is $\omega = 2\Omega \sin(ka/2)$. Henceforth, the *k* subscript that appeared earlier on $\omega_k$ and $C_k$ is dropped, replaced by $\omega(k)$ and $C(k)$, as all distributions in *k* and $\omega$ spaces will be treated as continuous.

[2] It is not problematic in the present context, but it is often the case that one should be cautious when referring to the dimension of a space. It would usually be more appropriate to replace the word dimension with direction. The reason for the distinction is that the spin of an elementary fermion such as the electron requires a 3D space. In 2D there is no spin-statistics connection of the kind that gives the Pauli exclusion principle. Frank Wilczek worked this out and assigned the term anyons to such elementary 2D particles.

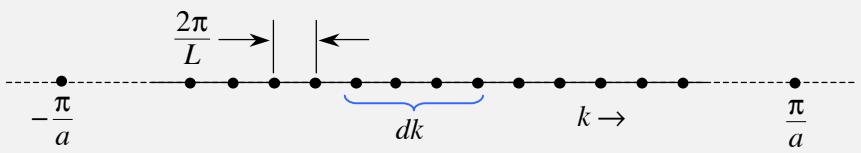


Figure 2. Allowed $k$ values are indicated with black dots. For a 1D monatomic lattice, the separation between adjacent $k$-values is equal to $2\pi / L$. In a small interval $dk$, the number of $k$ values is equal to $\rho_1(k)dk$, where $\rho_1(k)$ is the density of $k$ values. It is necessary to satisfy $dk >> 2\pi / L$ if we are to have an effectively continuous $k$-space density $\rho_1(k)$. Note that integration of $\rho_1(k)dk$ over the range $-\pi / 2 \le k \le \pi / 2$ yields the number of modes, $N$.

To proceed, the fact that a given number of modes can be expressed in either $\omega$-space or $k$-space, that is, $g_1(\omega)d\omega = \rho_1(k)dk$ (see Fig. 3), is used to write

$$g_1(\omega) = \rho_1(k)\left(\frac{dk}{d\omega}\right). \tag{2.11}$$

We shall first obtain $dk / d\omega$ and then combine this with $\rho_1(k)$ to obtain $g_1(\omega)$.

For spaces of any dimension (1D, 2D, or 3D), when obtaining $g(\omega)$ it is understood that the $k$ that appears in the $k$-space density $\rho(k)$ is to be replaced with a function of $\omega$. Specifically, $k$ is replaced with $k(\omega)$ according to the dispersion relation. In the 1D case under consideration, $\rho_1(k)$ is constant ($L/2\pi$), so this substitution does not arise. We simply replace $\rho_1(k)$ with $L/2\pi$. The next section deals with a 3D case, where the issue is revisited because $\rho_3(k)$ is proportional to $k^2$. Note that the parenthetic term on the right hand side of eqn (2.11) is the inverse of the group velocity: $v_g \equiv \partial\omega / \partial k$.

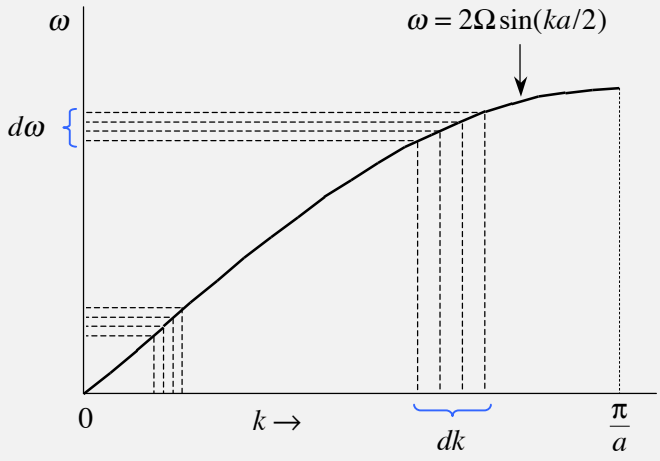


Figure 3. The interval $dk$ is mapped onto the interval $d\omega$ through the dispersion relation given at the top. As the edge of the Brillouin zone is approached along the dispersion curve, the slope flattens and therefore the density of $\omega$ values increases. At low $k$, the linear relationship between $\omega$ and $k$ (dashed lines in lower left) gives the speed of sound, $\omega = vk$.

Differentiation of the dispersion relation $\omega = 2\Omega\sin(ka/2)$ yields

$$\frac{dk}{d\omega} = \frac{1}{\Omega a\cos(ka/2)}. \tag{2.12}$$

Putting this into eqn (2.11), and using $\rho_1(k) = L/2\pi$, yields

$$g_1(\omega) = \frac{L}{2\pi}\frac{1}{\Omega a\cos(ka/2)}. \tag{2.13}$$

As usual, $k$ spans the $2\pi/a$ range that is symmetric about $k = 0$: $-\pi/a \le k \le \pi/a$. Keep in mind that the $k$ that appears on the right hand side of eqn (2.13) is to be replaced with a function of $\omega$ according to the dispersion relation. Writing the right hand side of eqn (2.13) in terms of $\omega$ is generally awkward and offers no clear advantage. Thus, we will stick with eqn (2.13) as it stands, with the understanding that the $\omega$ dependence of the right hand side is obtained through the dispersion relation $\omega = 2\Omega\sin(ka/2)$.[3] To obtain $g_1(\omega)$ in terms of only positive $k$ values, simply multiply the right hand side of eqn (2.13) by two.

The expression for $g_1(\omega)$ given by eqn (2.13) has the interesting feature that it goes to infinity when $\cos(ka/2) = 0$ at the edge of the first Brillouin zone. However, there is no cause for alarm. We know that this mathematically singular behavior cannot result in something strange happening, because in 1D the number of modes is equal to $N$. In other words, integrating $g_1(\omega)d\omega$ and $\rho_1(k)dk$ must yield $N$ in both cases. The singularity that appears in eqn (2.13) is said to be integrable.[4]

---

[3] In the present example, an expression for $\cos(ka/2)$ is readily obtained from the dispersion relation $\omega = 2\Omega\sin(ka/2)$:

$$\left(\frac{\omega}{2\Omega}\right)^2 = \sin^2(ka/2) = 1-\cos^2(ka/2) \implies \cos(ka/2) = \sqrt{1-\left(\frac{\omega}{2\Omega}\right)^2} = \frac{1}{2\Omega}\sqrt{4\Omega^2-\omega^2}.$$

Thus, eqn (2.13) can be written: $g_1(\omega) = \frac{L}{a}\frac{1}{\pi}\frac{1}{\sqrt{4\Omega^2-\omega^2}} = \frac{N}{\pi}\frac{1}{\sqrt{4\Omega^2-\omega^2}}$.

Using positive $k$, the integral of $2g_1(\omega)$ (note that the factor of 2 is needed to account for the negative $k$ values) over $\omega$ yields $N$, as expected. As mentioned in the text, writing $g_1(\omega)$ in this form offers no clear advantage.

[4] Integration in $k$-space yields the number of modes: $2\int_0^{\pi/a} dk\rho_1(k) = 2\frac{\pi}{a}\frac{L}{2\pi} = \frac{L}{a} = N$.

Likewise: $\int d\omega\, g(\omega) = \int d\omega \frac{L}{2\pi}\frac{1}{\Omega a\cos(ka/2)}$. Using $\omega = 2\Omega\sin(ka/2)$ again yields $N$.

## Example 2.1. Driven Classical Oscillator with Loss

The driven 1D classical harmonic oscillator with loss is a common and useful pedagogical model that is germane to a number of areas. In the present context, the driving force might be thought of as due to the presence of electromagnetic radiation whose frequency is in near-resonance with some optical phonon frequencies. For example, suppose laser radiation is used to excite modes in an optical branch. If the radiation is of a continuous nature (for example, a continuous wave laser as opposed to a pulsed laser), information can be obtained through a frequency domain measurement such as an absorption spectrum. Alternatively, if the radiation is contained in a sufficiently short duration pulse (say, in the femtosecond regime), important dynamical processes will transpire subsequent to photoexcitation. In this latter case, measuring the system's time domain response is likely to be the preferred means of interrogation.

When an optical branch phonon is removed (deactivated), phonons can be created concomitantly in the same and other optical branches, and in the acoustic branches. The parallel to be drawn with the present example is between the decay of an excited state in the phonon case, and the dissipation that takes place in a single classical oscillator that is deactivated through a frictional force. A relationship will emerge between time and frequency domain manifestations that carry over, to a large extent, to the quantum regime. Analysis of the quantum case is more demanding mathematically, so we will not get to it here. The math is not terrible, but it is time consuming and we lack the time. However, much if not most of the important understanding can be gleaned from the classical case.

To begin, a sinusoidal driving force of frequency $\omega$ is assumed to act on a particle that would, in the absence of the frictional force, undergo simple harmonic oscillation, *i.e.*, there are no anharmonic terms in the potential energy function. However, the particle experiences a frictional force that is proportional to its speed, and therefore its equation of motion is

$$m\ddot{x} + b\dot{x} + \kappa x = Fe^{i\omega t} . \qquad (i)$$

The constant $F$ needs to be complex if we wish to keep track of the phase of the driving force, *e.g.*, $F = F_{real}\, e^{i\varphi}$ , where $\varphi$ is the phase of the driving force. However, this is usually unimportant, in which case $F$ can be taken as real. The real constant $b$ accounts for loss in the form of friction. The simplest example of such frictional force that comes to mind is that of an object falling toward the earth through the earth's atmosphere. For example, think of a cantaloupe released from a small plane 4000 meters above the ground. It reaches a constant speed that balances the frictional force presented by the atmosphere with the gravitational force. The resulting speed is $\dot{x} = ma/b$ , where $a$ is the gravitational acceleration near the earth's surface.

Dividing eqn (*i*) by the particle mass $m$ yields the equation that is to be solved:

$$\ddot{x} + 2\beta\dot{x} + \omega_0{}^2 x = Ae^{i\omega t} . \qquad (ii)$$

The parameter $\beta = b/2m$ is introduced to simplify the manipulations that follow, and $\omega_0{}^2 = \kappa/m$. As usual, it is understood that the real part is taken at the end.

There are two parts to the solution of eqn (*ii*), a driven part that is due solely to the right hand side, $Ae^{i\omega t}$, and a homogeneous part that satisfies eqn (*ii*) with the right hand side set equal to zero. We shall first obtain the driven solution and then add the transient part, that is, the solution of the homogeneous equation. At the end, initial conditions are used to assign values to the integration constants.

Next, $x = x_0 e^{i\omega t}$ is introduced. This is a statement that the driven solution must oscillate at the frequency of the driving force after all transients have decayed to zero. The constant $x_0$ is complex because in general there is a phase difference between the driving force and the system's response. Introducing $x = x_0 e^{i\omega t}$ into eqn (*ii*) yields the algebraic equation

$$\left(-\omega^2 + i2\beta\omega + \omega_0{}^2\right) x_0 e^{i\omega t} = Ae^{i\omega t} . \qquad (iii)$$

The exponential terms $e^{i\omega t}$ cancel (red lines), leaving

$$x_0 = \frac{-A}{\omega^2 - \omega_0{}^2 - i2\beta\omega} \qquad (iv)$$

$$= \frac{-A}{(\omega + \tilde{\omega} - i\beta)(\omega - \tilde{\omega} - i\beta)} , \qquad (v)$$

where $\tilde{\omega}^2 = \omega_0{}^2 - \beta^2$, which is easily verified by substitution. Let us now enlist the fact that we are interested in driving the system near one of its resonances. In this case, $\omega$ is close to either $+\tilde{\omega}$ or $-\tilde{\omega}$. Obviously it cannot be near each at the same time. It is also assumed that the frictional loss parameter $\beta$ is small relative to the oscillation frequencies. In other words, we are interested in resonances that are fairly sharp. These assumptions enable us to use the approximation $\tilde{\omega} \approx \omega_0$. Choosing the $\omega \approx +\omega_0$ option, eqn (*v*) becomes

$$x_0 = -\frac{A}{2\omega_0}\frac{1}{\omega - \omega_0 - i\beta} . \qquad (vi)$$

$$= -\frac{A}{2\omega_0}\left(\frac{\omega - \omega_0}{(\omega - \omega_0)^2 + \beta^2} + i\frac{\beta}{(\omega - \omega_0)^2 + \beta^2}\right) . \qquad (vii)$$

Taking the real part of $x = x_0 e^{i\omega t}$ yields the driven (steady-state) solution. The solution to the homogeneous equation (the transient solution) is added to the steady state solution to obtain the final result:

$$x = \mathrm{Re}\left(x_0 e^{i\omega t} + x_{\text{transient}}\right) \qquad (viii)$$

$$= -\frac{A}{2\omega_0}\frac{1}{(\omega-\omega_0)^2+\beta^2}\left((\omega-\omega_0)\cos\omega t-\beta\sin\omega t\right)$$

$$+\ e^{-\beta t}\left(C_1\cos\omega_0 t + C_2\sin\omega_0 t\right). \qquad (ix)$$

It is understood that the $x$ on the left hand side of eqns (*viii*) and (*ix*) refers to $\mathrm{Re}(x)$. Hereafter, $x$ will be used to represent $\mathrm{Re}(x)$. As mentioned earlier, the constants $C_1$ and $C_2$ are determined by the initial conditions.

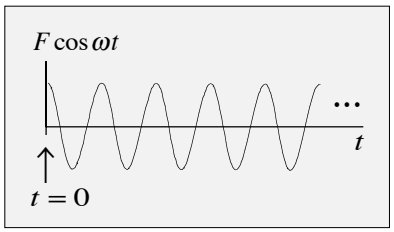


Immediately following excitation with a sinusoidal driving force that remains on for a long time after it has been switched on at $t$ = 0 (see the box on the right), there is a transient. This transient decays with an exponential lifetime of $\beta^{-1}$, leaving just the steady-state response. At exact resonance ($\omega = \omega_0$), and after any transients have decayed to zero, $x$ is equal to $(A/2\beta\omega_0)\sin\omega_0 t$. As expected, both the displacement amplitude $x$ and the speed $\dot{x}$ vary inversely with the frictional loss parameter $\beta$. For example, notice that as the loss goes to zero, $x$ and $\dot{x}$ each goes to infinity. This is not surprising, however, because the model is unphysical in the sense that the displacement and speed must increase without bound for a driven system without loss. All physical systems have some degree of loss (coupling to something they perceive as exterior), so think of this divergence as just one of those things that happens from time to time with mathematical models.

A sinusoidal driving force has been used in the above example. However, an arbitrary driving force can be expressed mathematically using a Fourier expansion. For example, think of a repetitive driving force comprised of harmonics of a driving force's fundamental frequency. Equation (*ii*) then becomes many equations, namely, one for each harmonic. The solutions to these equations follow straightforwardly. They are essentially the same as for the case of a single driving frequency, but with different frequencies.

If the driving force is absent, we are left with just the transient response. For example, with $\dot{x}$ = 0 at $t$ = 0 we have $x(t) = C_1 e^{-\beta t}\cos\omega_0 t$. This is a rapid oscillation whose envelope is damped exponentially. To see what this looks like in the frequency domain, take the Fourier transform of $x(t)$. Suppressing all constants, this is given by

$$X(\omega) = \int_0^\infty dt\, e^{-i\omega t}e^{-\beta t}\left(e^{i\omega_0 t}+e^{-i\omega_0 t}\right) \qquad (x)$$

$$= \frac{-i}{(\omega-\omega_0)-i\beta}+\frac{-i}{(\omega+\omega_0)-i\beta}. \qquad (xi)$$

The second term is negligible as long as we restrict frequencies to $\omega \approx \omega_0$. There are several complementary ways to view this result. Perhaps the simplest is to note that its squared modulus is proportional to a Lorentzian lineshape, as shown on the right. For $\omega \approx \omega_0$, eqn (*xi*) reduces to a single complex entity (the first term on the right hand side) that can be expressed in terms of its real and imaginary parts:

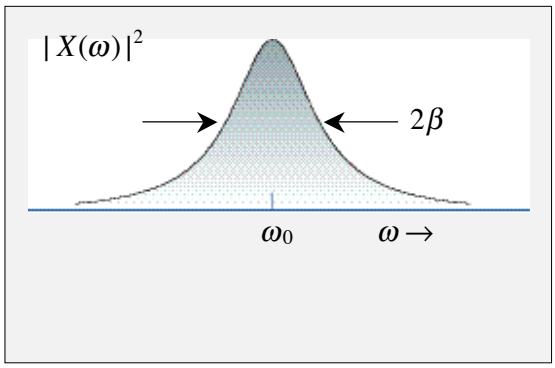


$$X(\omega) = \frac{\beta^2}{(\omega-\omega_0)^2+\beta^2} - i\frac{(\omega-\omega_0)}{(\omega-\omega_0)^2+\beta^2}.$$

And so on.

## 2.5. Three-Dimensional Lattice

Let us now extend $g_1(\omega_k)$ from 1D to 3D. Again, we shall start with the density in *k*-space, but this time for a 3D volume element

$$\rho_3(k_x,k_y,k_z)\,d^3k = (L_xL_yL_z/(2\pi)^3)\,dk_x\,dk_y\,dk_z\,. \tag{2.14}$$

It is a safe assumption that the heat capacity of a crystal does not depend on its shape.[5] Therefore, $L_xL_yL_z = V$ is used. Now replace $dk_x\,dk_y\,dk_z$ with the spherical volume element: $k^2\sin\theta\,d\theta\,d\phi\,dk$. Integration over $\theta$ and $\phi$ yields $4\pi$, which gives $\rho_3(k)\,dk = (V/2\pi^2)\,k^2dk$. Thus, for 3D, $g(\omega)$ is

$$\boxed{g(\omega) = \frac{V}{2\pi^2}k^2\frac{dk}{d\omega}\,,} \tag{2.15}$$

where $dk/d\omega$ is evaluated using the dispersion relation.

The $g(\omega)$ in eqn (2.15) is the 3D counterpart to $g_1(\omega)$ in eqns (2.11) and (2.13). It refers to a single branch of the dispersion relation. To include all participating branches, we simply add their contributions. This includes the optical branches in addition to the acoustic branches. Optical branches are important when $k_BT$ is comparable to or exceeds the optical phonon frequencies. We shall avoid the math required to deal directly with the inclusion of the optical branches by using the Debye model, as described below.

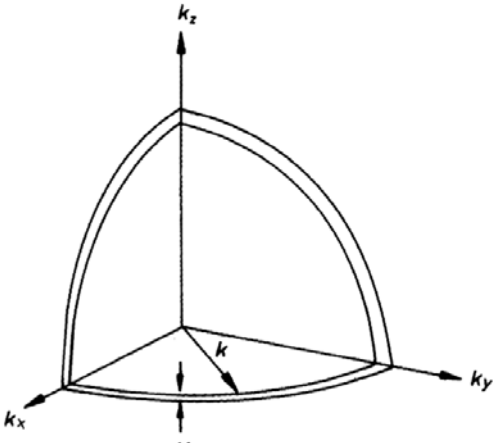


Figure 4. The differential volume element in *k*-space is a thin spherical shell of thickness *dk* (from Hook and Hall).

Referring to Fig. 4, it is understood that *k* is positive because it is the radial distance in *k*-space. As mentioned earlier, the subscript *k* on $\omega_k$ is no longer needed, as frequency and wave vector are, for all practical purposes, continuous variables. This is implicit in eqn (2.15), where we write $dk/d\omega$. The term $dk/d\omega$ is obtained from the dispersion relation. The average energy of the sample at temperature *T* is obtained by integrating the product of $g(\omega)$ given by eqn (2.15) times the average energy contained in each mode at temperature *T*. This latter quantity is $\omega_k$ times $\langle n_k \rangle$ given

[5] A crystal's thermal conductivity in general varies, often strongly, with the direction of heat flow. On the other hand, in the absence of a thermal gradient, energy density is constant to a high degree of accuracy throughout the crystal, influenced only by the crystal edges.

by eqn (2.7), though now the subscripts are dropped and $\hbar = 1$ is used. Integration is over all modes. Putting all of this together, the average stored energy is given by

$$\langle E \rangle = \int_0^\infty d\omega \left( \frac{\omega}{e^{\omega/k_B T} - 1} \right) g(\omega) \tag{2.16}$$

These are restricted to the first Brillouin zone.

$$= \frac{V}{2\pi^2} \int_0^\infty d\omega \left( \frac{\omega}{e^{\omega/k_B T} - 1} \right) k^2 \frac{dk}{d\omega} . \tag{2.17}$$

The function $g(\omega)$ is truncated at some maximum value in accord with $k$ being restricted to the first Brillouin zone. This establishes the upper integration limit. In other words, the limit of infinity in eqn (2.16) is never reached. It is retained however (with the limit imposed by the first Brillouin zone understood), because it simplifies some of the integrations encountered below.

As mentioned above, though not indicated explicitly, the integration in eqn (2.17) is carried out over all branches. In other words, there are separate integrations for each branch because a separate $g(\omega)$ applies to each branch. If the crystal is monatomic (a single spring constant), there are three integrals, one for each of the acoustic branches. With less simple crystals, optical branches enter. In general, dispersion relations cannot be expressed in closed form, and they can be complicated. Thus, we can appreciate why an accurate calculation could prove arduous, perhaps not as a research project, but certainly as a classroom exercise.

From eqn (2.16), it is easy to see what happens at high temperature. You probably have encountered the high-$T$ limit before, say, in undergraduate physical chemistry. The contents of the large parentheses reduces to $k_B T$, and eqn (2.16) becomes

$$\langle E \rangle = k_B T \int_0^\infty d\omega \, g(\omega) . \tag{2.18}$$

The value of the integral is, by definition, $3N$ for a monatomic 3D lattice. That is, $N$ atoms have $3N$ degrees of freedom that result in $3N$ vibrational modes. Thus, differentiation of $\langle E \rangle$ with respect to $T$ gives a simple expression for the high temperature limit of the heat capacity:

$$\boxed{C = 3N k_B \quad \text{high-}T \text{ limit}} . \tag{2.19}$$

This result also follows from the fact that, classically, each vibrational degree of freedom contributes $k_B$ to the heat capacity, and there are $3N$ degrees of freedom. The heat capacity given by eqn (2.19) is twice as large as for a gas comprised of $N$ atoms. The difference is due to the fact that vibrational energy varies quadratically with both momentum and displacement, whereas a gas has only the momentum contribution.

Turning to the low temperature limit, we now invoke the fact that the acoustic dispersion curves are linear in this regime, with speeds of sound $v_{\mathrm{L}}$, $v_{\mathrm{T}_1}$, and $v_{\mathrm{T}_2}$ for the longitudinal and two transverse branches, respectively. Using this with eqn (2.17) yields

$$\langle E \rangle = \frac{V}{2\pi^2}\underbrace{\left(\frac{1}{{v_{\mathrm{L}}}^3}+\frac{1}{{v_{\mathrm{T}_1}}^3}+\frac{1}{{v_{\mathrm{T}_2}}^3}\right)}_{\text{sum over 3 acoustic branches}}\int_0^\infty d\omega\,\frac{\omega^3}{e^{\omega/k_BT}-1}\,. \tag{2.20}$$

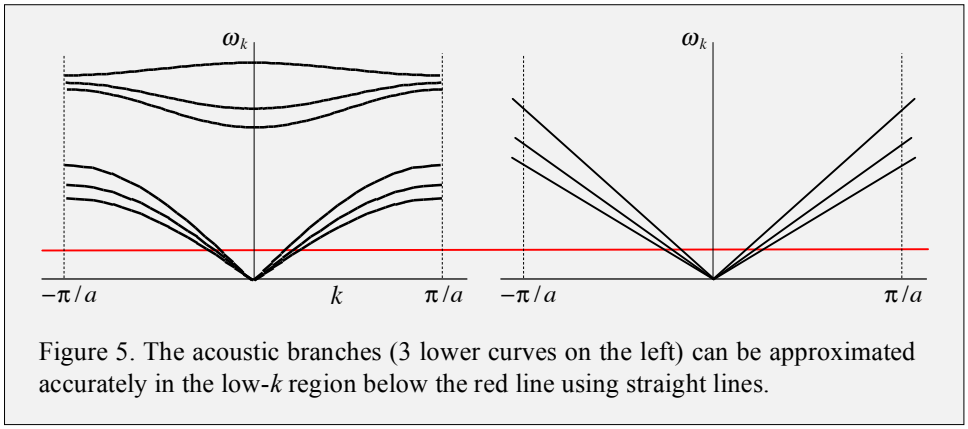


Figure 5. The acoustic branches (3 lower curves on the left) can be approximated accurately in the low-*k* region below the red line using straight lines.

Figure 5 illustrates the use of the linear portions of the three acoustic branches. The upper integration limit of infinity is acceptable because high frequency modes do not participate at low temperatures. In the spirit of keeping things simple, the large parenthetic term in eqn (2.20) is replaced by $3v^{-3}$. You can think of this as an average value of the inverse cube of the speed of sound in the acoustic branches, or, equivalently, that we are assuming that the speed of sound is the same for each of the branches. In any event, using $3v^{-3}$ and the substitution $x = \omega / k_BT$, eqn (2.20) becomes

$$\langle E \rangle = \frac{V}{2\pi^2}\frac{3}{v^3}\frac{(k_BT)^4}{\hbar^3}\int_0^\infty dx\,\frac{x^3}{e^x-1}\,. \tag{2.21}$$

Note that explicit $\hbar$ has now been introduced. The value of the integral is $\pi^4/15$, and differentiation with respect to $T$ gives the heat capacity for the low temperature limit

$$C = 3.95\left(\frac{k_BV}{v^3}\right)\left(\frac{k_BT}{\hbar}\right)^3 \quad \text{low-}T\text{ limit}\,. \tag{2.22}$$

This model of the low temperature limit holds up well against experimental data. Figure 6 shows the result obtained by carrying out heat capacity measurements for a

monatomic lattice of argon atoms. The temperature range is low indeed, not exceeding 2 K. The agreement between experiment and theory is stunning.

The limiting cases discussed above are straightforward. Let us now examine the full temperature range by using the model introduced by Debye. This model has great value because it enables one to judge material properties on the basis of parameters that can be obtained from experiment. It is an interpolation that gets around the mathematical task that would be faced were we to deal directly with the optical modes.[6]

Figure 6. Heat capacity in units of $\mathrm{mJ \cdot mol^{-1} \cdot K^{-1}}$: experimental result for a monatomic lattice of solid argon at temperatures < 2 K. The data follow the predicted $T^3$ dependence very well (from Kittel, *Introduction to Solid State Physics* [5], who references L. Finegold and N. E. Phillips, for the data shown on the right).

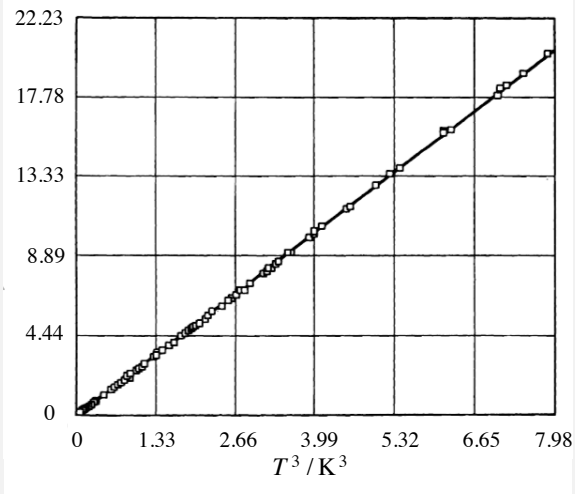


Keep in mind that dispersion relations in general can be complicated, depending on what goes into a primitive unit cell, crystal symmetry, and so on. Figure 7 shows the case of a diatomic lattice of a typical face-centered cubic crystal. This is still relatively simple, yet we see changes from the dispersion relations introduced so far. For example, one optical branch increases with wave vector while the other decreases with wave vector, and two of the LA acoustic branches are of different character than those introduced so far. Notice that some of the curves cross in *k*-space.

[6] A convenient and accurate algorithm for dealing with many vibrational degrees of freedom is the one introduced by Beyer and Swinehart [75]. It is used frequently to estimate level densities in statistical theories of unimolecular reactions.

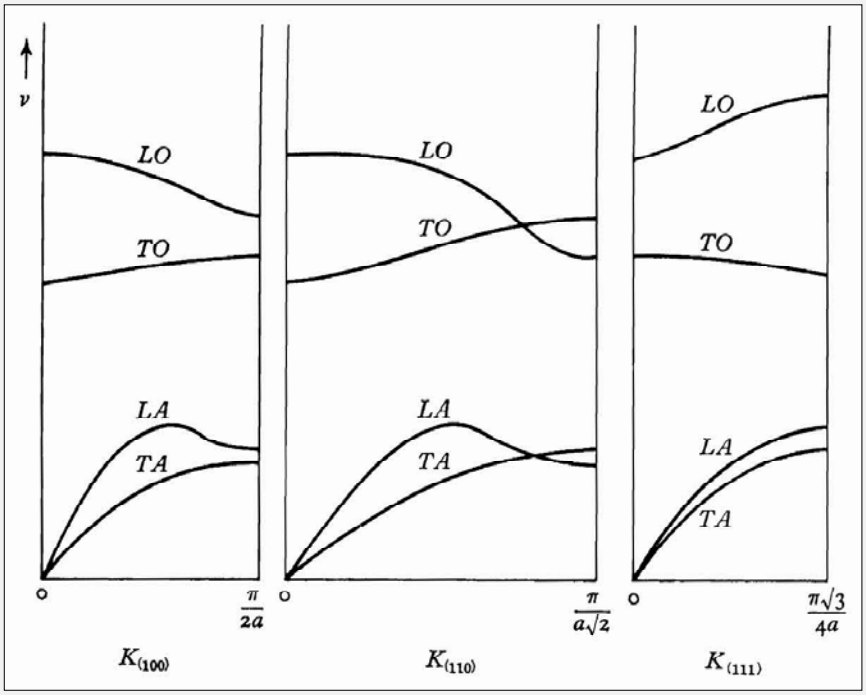


Figure 7. From Sherwood: *Vibrational Spectroscopy of Solids*. Note that for the (100), (110), and (111) directions, the transverse phonons are doubly degenerate.

## 2.6. Debye Model


Peter Debye

In the simplest version of the Debye model, the speed of sound is assigned the same value in each of three acoustic branches, and the dispersion relation is taken to be a straight line: $\omega = vk$. There is no flattening of the $\omega(k)$ curve as $k$ approaches the edge of the Brillouin zone. The optical branches are not included explicitly. Their effect insofar as heat capacity is subsumed into the dispersion relation $\omega = vk$.

The relation $\omega = vk$ is taken as valid up to some cutoff frequency, $\omega_D$, that is referred to as the Debye frequency, above which there are no available modes. The cutoff wave vector associated with $\omega_D$ is $k_D = \omega_D / v$. We shall see that $k_D$ lies within the Brillouin zone, not at its edge. This construct might sound bizarre, because you have learned that dispersion curves, even for the acoustic branches, are never so simple. Or are they?

The flattening of the $\omega(k)$ curve as $k$ approaches the edge of the Brillouin zone is a consequence of the discrete nature of the lattice. Were the medium completely elastic with harmonic restoration, and with no hint of an underlying lattice structure, there could be neither the above flattening nor optical branches. We shall return to this situation later and see that it represents some very important systems. For the case at hand, the Debye ansatz ensures a model that is exact in the high and low frequency limits. In other words, it is an interpolation between these limiting cases. Therefore it might have problems in the intermediate regime. Nonetheless, it serves as a reasonable first estimate, or at least a pedagogical exercise on the way to more advanced models.

The cutoff frequency $\omega_D$ is obtained by using the fact that the integral of $g(\omega)d\omega$ from 0 to $\omega_D$, by definition, gives the number of modes in 3D space. Equivalently, integration of the $k$-space density from $k = 0$ to $k_D$ must also give the number of modes. We shall now use $g(\omega)$ to obtain $\omega_D$, in which case integration is carried out in frequency space. For $N$ atoms, there are $3N$ modes. Introducing the above assumptions into eqn (2.15) and integrating $g(\omega)d\omega$ yields:

$$3N = \int_0^{\omega_D} d\omega\, g(\omega) \tag{2.23}$$

Using $g(\omega) = \rho(k)(dk/d\omega)$ and eqn (2.15) gives

$$3N = \frac{V}{2\pi^2} \int_0^{\omega_D} d\omega \underbrace{3k^2 \frac{dk}{d\omega}}_{3(\omega^2/v^3)} \qquad \text{3 acoustic branches} \tag{2.24}$$

$$= \frac{V}{2\pi^2}\frac{3}{v^3}\int_0^{\omega_D} d\omega\, \omega^2 \tag{2.25}$$

Thus, $\omega_D{}^3 = v^3 6\pi^2 N/V$ and $k_D{}^3 = 6\pi^2 N/V$. The parameters $\omega_D$ and $k_D$ are seen to have quite simple forms:

$$\boxed{\omega_D = v k_D = v(6\pi^2 n)^{1/3},} \tag{2.26}$$

where $n = N/V$ is the number of atoms per unit volume.

An alternate way to arrive at this result is to use the volume of a *k*-space sphere having a radius of $k_D$, namely $4\pi k_D{}^3/3$. It is assumed that all modes are contained within this sphere. Namely, they fill *k*-space up to the sphere's edge but not beyond. Dividing the volume $4\pi k_D{}^3/3$ by the *k*-space volume of a single *k*-space cell: $(2\pi)^3/V$, gives the number of modes per branch. Multiplying this number by 3 accounts for the 3 branches.

Combining the above items and using the fact that there are $3N$ modes gives

$$3N = \left(\frac{4\pi}{3}k_D{}^3\right)\left(\frac{3V}{(2\pi)^3}\right) = \frac{3V}{6\pi^2}k_D{}^3 \tag{2.27}$$

Thus, $k_D = (6\pi^2 n)^{1/3}$, which is eqn (2.26). The only free parameter in the model is the speed of sound – equivalently the Debye frequency: $\omega_D = v(6\pi^2 n)^{1/3}$. This can be taken from independent measurements or adjusted to fit data. However, it should not deviate much from the known speed of sound in the material.

Now that we have the Debye cutoff frequency $\omega_D$, the heat capacity is obtained in a few steps starting with eqn (2.17). Note that the right hand side of eqn (2.17) needs to be multiplied by 3 to account for the 3 acoustic branches. With the upper integration limit set at $\omega_D$, eqn (2.17) becomes

$$\langle E \rangle = \frac{3V}{2\pi^2}\int_0^{\omega_D} d\omega \left(\frac{\omega}{e^{\omega/k_BT}-1}\right) k(\omega)^2 \frac{dk(\omega)}{d\omega}. \tag{2.28}$$

With the Debye ansatz, $\omega = vk$, the heat capacity is given by

$$C = \frac{3V}{2\pi^2 v^3}\frac{\partial}{\partial T}\int_0^{\omega_D} d\omega \left(\frac{\omega^3}{e^{\omega/k_BT}-1}\right). \tag{2.29}$$

To evaluate the right hand side, take the derivative and carry out the integration. The steps are given in the box below. Also, let us express the heat capacity as a per unit volume quantity by dividing the right hand side of eqn (2.29) by the volume *V*. The same symbol *C* is used, hopefully without confusion. The resulting expression is

$$C = 9nk_B\left(\frac{T}{\Theta_D}\right)^3 \int_0^{x_D} dx\left(\frac{x^4 e^x}{(e^x-1)^2}\right), \tag{2.30}$$

where $\Theta_D = \omega_D / k_B$ and $x = \omega / k_B T$.

This result is general in the sense that it is valid for any temperature. The parameter $\Theta_D$ can be obtained from experimental measurements. It is used frequently as a rough measure of the stiffness of a crystal. Values for alkali halide ionic crystals are given in Table 1, and values for crystals made of atoms are given in Table 2.

Using $\omega_D{}^3 = 6\pi^2 v^3 (N/V)$, eqn (2.29) becomes: $C = \frac{9N}{\omega_D{}^3}\int_0^{\omega_D} d\omega\,\omega^3 \frac{\partial}{\partial T}\left(\frac{1}{e^{\omega/k_BT}-1}\right)$

Next, carry out a couple of operations:

$$C = \frac{9N}{\omega_D{}^3}\int_0^{\omega_D} d\omega\,\omega^3\left(\frac{(\omega/k_BT^2)e^{\omega/k_BT}}{(e^{\omega/k_BT}-1)^2}\right) = \frac{9N}{\omega_D{}^3}\frac{1}{k_BT^2}\int_0^{\omega_D} d\omega\left(\frac{\omega^4 e^{\omega/k_BT}}{(e^{\omega/k_BT}-1)^2}\right)$$

With $x = \omega / k_B T$, this becomes:

$$C = \frac{9N}{\omega_D{}^3}\frac{(k_BT)^5}{k_BT^2}\int_0^{x_D} dx\left(\frac{x^4 e^x}{(e^x-1)^2}\right) = 9Nk_B\left(\frac{k_BT}{\omega_D}\right)^3 \int_0^{x_D} dx\left(\frac{x^4 e^x}{(e^x-1)^2}\right)$$

Using the definition of the Debye temperature: $\Theta_D = \omega_D / k_B$, the above expression becomes:

$$C = 9Nk_B\left(\frac{T}{\Theta_D}\right)^3 \int_0^{x_D} dx\left(\frac{x^4 e^x}{(e^x-1)^2}\right) \xrightarrow{\div V} C = 9nk_B\left(\frac{T}{\Theta_D}\right)^3 \int_0^{x_D} dx\left(\frac{x^4 e^x}{(e^x-1)^2}\right)$$

In the high temperature limit the integral is evaluated by noting that the exponential in the numerator is equal to one, while the denominator is equal to $x^2$ because $e^x \to 1 + x$. The integrand is therefore $x^2$, and integration yields $x^3/3$. Thus, we see that the high temperature limit of eqn (2.30) is $C = 3nk_B$, which is recognized as the classical limit of the heat capacity for a crystal comprised of $N$ particles (*i.e.*, $3N$ oscillators) in a volume $V$. Recall eqn (2.19).

The low temperature limit also follows straightforwardly from eqn (2.30). In this case, the upper integration limit is set at infinity for convenience. This works because the occupied modes are nearly all contained in the low-$k$ region at low temperature, so the usual limit of restriction to the first Brillouin zone can be relaxed, and $k$ can be allowed to go to infinity. The integral in eqn (2.30) is one of those things that happen every so often. I am not going to discuss its evaluation. The final result is that the heat capacity is

Table 1. Debye temperatures ($\Theta_D$) for alkali halide crystals

| | F | Cl | Br | I |
|---|---|---|---|---|
| Li | 730 | 422 | — | — |
| Na | 492 | 321 | 224 | 164 |
| K | 336 | 231 | 173 | 131 |
| Rb | — | 165 | 131 | 103 |

$$C = 234\, n k_B \left(\frac{T}{\Theta_D}\right)^3 \quad \text{low-}T\text{ limit} \tag{2.31}$$

Figure 8 shows a plot of the general expression for the heat capacity according to the Debye model [the left entry is a plot of eqn (2.30)] and experimental results for Si and Ge. Agreement between experiment and theory is very good. You can see this for germanium because I altered the horizontal scale in the figure I took from Kittel. Though less obvious, silicon also agrees, albeit over a smaller range.

Table 2. Debye temperatures ($\Theta_D$) for elements

| | | | | | | | | | |
|---|---|---|---|---|---|---|---|---|---|
| Li | 400 | Be | 1000 | B | 1250 | C | 1860 | As | 285 |
| Na | 150 | Mg | 318 | Al | 394 | Si | 625 | Sb | 200 |
| K | 100 | Ca | 230 | Ga | 240 | Ge | 360 | Bi | 120 |
| | | | | In | 129 | Sn | 260 | | |
| | | | | Tl | 96 | Pb | 88 | | |

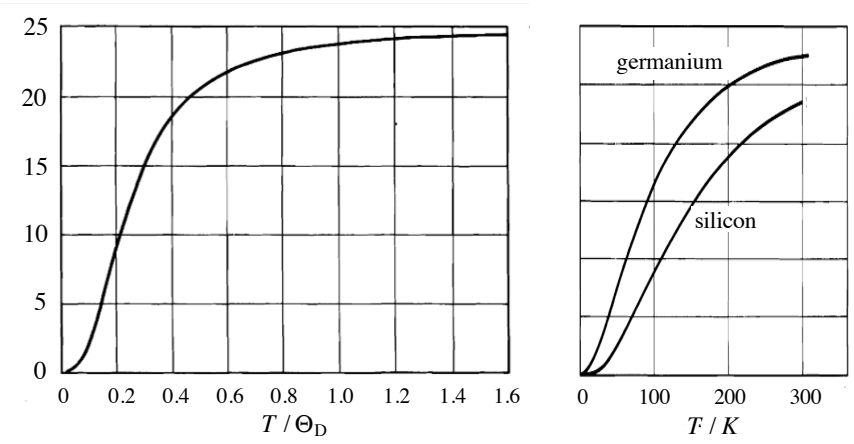


Figure 8. Left: calculated heat capacity versus $T/\Theta_D$ using eqn (2.31). Right: data for silicon and germanium follow Debye-like curves, assuming appropriate scale changes for horizontal axis (adapted from Kittel).

## 2.7. Thermal Conductivity

The remainder of Chapter 2 deals with thermal conductivity. This might sound like a boring subject, a leftover from the dark ages of classical thermodynamics. In fact, it is both scientifically challenging and of enormous technological importance. The number of areas in which thermal conductivity plays an important role is huge. We cannot begin to cover them here. In the next few sections, several fundamental aspects that are germane to a wide range of crystalline media will be introduced and examined.

We shall begin by considering the fact that the thermal conductivity of a perfectly harmonic crystal is infinite. Phonon wave packets can flow throughout such a crystal without changing their composition. They might broaden, distort, etc., but they remain composed of the same distribution of $k$ values that they began with. There is no mechanism for excitation to be transferred among the various normal modes. Consequently, heat can flow in the absence of a temperature gradient, which does not happen except in superfluid media, well known examples around here being superconductivity and liquid helium nanodroplets, which cool spontaneously to $\sim 0.4$ K.

Aside from scattering by defects, impurities, and surfaces, the only mechanism for wave vector change is anharmonicity, which, by definition, is absent in a perfectly harmonic crystal. The anharmonic parts of the potential that are important are those that couple the normal modes to one another. This is akin to the well-known couplings that exist in molecules, such as Fermi resonances, Darling-Dennison resonances, and so on. In dealing with anharmonicity in crystalline lattices, it will be seen that things can get complicated but at the same time quite interesting.

In Section 2.8 (immediately below), a simple expression will be derived for the thermal conductivity of a crystal in terms of heat capacity $C$, the speed of sound $v$, and a scattering parameter – either a scattering length $l$ or, equivalently, a scattering time $\tau$, where $l = v\tau$. We will find that a simple form is obtained, namely, $\kappa = Cvl/3$, where $\kappa$ is the thermal conductivity. The model is crude, but it contains sensible ingredients. The trickiest one is the scattering length $l$. Most of our time will be spent discussing this, finishing with the high and low temperature limits. As an interlude, we will explore an interesting phenomenon due to anharmonicity in a gas of carbon monoxide molecules. Time permitting this will be presented in one of our discussion sessions, so it is only outlined in these notes.

| Material | $\kappa$ $(\mathrm{W \cdot m^{-1} \cdot K^{-1}})$ |
|---|---|
| air | 0.025 |
| water (liquid) | 0.6 |
| water (ice) | 2 |
| concrete | 1.7 |
| glass | 1.1 |
| gold | 318 |
| lead | 35 |
| copper | 401 |
| silver | 429 |
| diamond | 900-2320 |

Thermal conductivity values: The large range for diamond is due to anisotropy.

## 2.8. Model Adapted from Gas Phase Kinetics

To begin, consider the energy per unit area per second that passes through a surface, as indicated in Fig. 9. It is assumed, with no loss of generality, that the surface normal lies parallel to the direction of heat flow. We seek an expression for the net flux in the direction of interest, namely, in the direction of the temperature gradient.

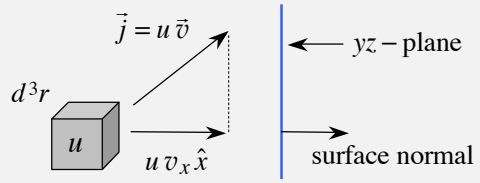


Figure 9. The energy contained in a small volume is $u\,d^3r$. It passes through the $yz$-plane (blue line). The flux $\vec{j}$ (whose units are $J \cdot m^{-2} \cdot s^{-1}$) is equal to $u\vec{v}$. Its component in the direction of the surface normal is $u\,v_x\hat{x}$.

The strategy that underlies this approach derives from gas phase kinetics. Referring to Fig. 9, $u$ denotes the energy density and $\vec{j}$ its corresponding flux, *i.e.*, $\vec{j} = u\vec{v}$. A small volume $d^3r$ containing the energy density $u$ is some distance from a surface that is nothing more than the $yz$-plane (solid blue line in Fig. 9, and dashed blue line in Fig. 10). The net flow of energy through this surface from the higher-temperature region to the lower-temperature region is the desired flux. It is assumed that temperature changes smoothly and monotonically in going from higher to lower temperature.

### Scattering Ansatz

Referring to Fig. 10, assume that the energy density $u$ is contained in a small volume that travels a length $l$ without scattering. This is akin to elementary gas phase kinetics theory, where a mean distance between collisions is invoked. Because the gradient of the energy density is in the $x$-direction, we write $u(x)$ to denote energy density as a function of distance along the $x$-axis. It is assumed that $u(x)$ does not vary in the $yz$-plane.

Figure 10. It is assumed that phonon wave packets travel, on average, a distance $l$ before making a "collision." Those that arrive at the black dot on the $yz$-plane (blue dashed line) originated on a sphere of radius $l$. The system has azimuthal symmetry about the $x$-axis. There are more phonons on the left than on the right, as these are the higher and lower-$T$ regimes, respectively. Thus, there is net flow of energy to the right.

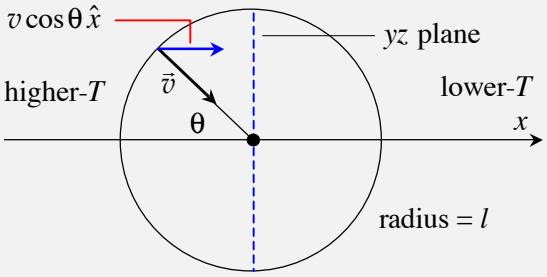


Figure 10 is a clever means of visualizing the flux that passes through a surface whose normal lies along the temperature gradient. To see how this works, consider a point in the $yz$-plane. This point is taken as the origin in the figure, and we ask the question: If energy

density moves a distance $l$ at speed $v$, where must it be located, and in what direction must it be traveling, in order that it reaches the origin after traveling the distance $l$?

Clearly, it must be distributed on a sphere of radius $l$ with velocities that point at the origin. This flow of energy contributes to the flux in the $x$-direction in proportion to the $x$-component of the velocity, $v_x = v\cos\theta$. Keep in mind that the *net* flux that passes through the blue plane is the difference between energy that passes from left to right (originates from the left hand side of the sphere) and energy that passes from right to left (originates from the right hand side of the sphere). The $x$-directed flux will be evaluated at the origin with the understanding that the result applies anywhere in the $yz$-plane. The net $x$-directed flux through the surface is obtained by averaging the product $v_x u(x) = v\cos\theta u(x)$ over the surface of the sphere:

$$j_x = \frac{1}{4\pi}\int_0^{2\pi} d\phi \int_0^{\pi} d\theta \sin\theta \; v\cos\theta u(x) . \tag{2.32}$$

Nothing depends on $\phi$, so integration over $\phi$ gives $2\pi$.

Next, to introduce the spatial variation of $u(x)$ in the direction of the temperature gradient, $u(x)$ is expanded in a Taylor series: $u(x) = u(0) + (\partial u/\partial x)_0 x \ldots$. The constant term in the expansion, $u(0)$, does not contribute to $j_x$ because there can be no net flux through the surface if the energy density is constant throughout space. The first non-vanishing term is what we will use, and this yields, using the substitution $x = -l\cos\theta$ (see Fig. 10):

$$j_x = \tfrac{1}{2} v \int_0^{\pi} d\theta \sin\theta\cos\theta \left( \left.\frac{\partial u}{\partial x}\right|_{x=0} \left(-l\cos\theta\right)\right), \tag{2.33}$$

where $(\partial u/\partial x)\big|_{x=0}$ is evaluated at the $x = 0$ location indicated by the origin in Fig. 10. It is implicit in the above that $l$ is smaller than the characteristic distance over which $u(x)$ changes significantly. Hereafter, the subscript on the term $(\partial u/\partial x)\big|_{x=0}$ shall be taken as understood. Thus, the expression for $j_x$ in eqn (2.33) becomes

$$j_x = -\tfrac{1}{2} v l \frac{\partial u}{\partial x} \int_0^{\pi} d\theta \sin\theta\cos^2\theta . \tag{2.34}$$

The integral is evaluated by using $d\theta\sin\theta\cos^2\theta = -d(\cos\theta)\cos^2\theta = -d\alpha\,\alpha^2$. Integration yields $2/3$. The term $\partial u/\partial x$ is equal to $(\partial u/\partial T)(\partial T/\partial x) = C(\partial T/\partial x)$. Thus, the expression for the $x$-directed flux becomes

$$j_x = \tfrac{1}{3} C v l \left(-\frac{\partial T}{\partial x}\right), \tag{2.35}$$

or

$$j_x = -\kappa \frac{\partial T}{\partial x}, \tag{2.36}$$

where $\kappa$ is the thermal conductivity:

$$\boxed{\kappa = \tfrac{1}{3} C v l .} \tag{2.37}$$

The $C$ in eqn (2.37) is the heat capacity. Its units are $\mathrm{J \cdot m^{-3} \cdot K^{-1}}$. Thus, thermal conductivity $\kappa$ has units $\mathrm{J \cdot m^{-1} \cdot s^{-1} \cdot K^{-1}}$ (equivalently $\mathrm{W \cdot m^{-1} \cdot K^{-1}}$), and the $x$-directed flux $j_x$ has units $\mathrm{J \cdot m^{-2} \cdot s^{-1}}$ (equivalently $\mathrm{W \cdot m^{-2}}$). As mentioned earlier, the tricky part is the scattering length. Let us now address this starting with crystal momentum.

## 2.9. Phonon Crystal Momentum

To understand how thermal conductivity works in an electrically insulating crystal, it is necessary to understand how "crystal momentum" (wave vector) transfer works in the crystal. We have seen that the concept of momentum in a periodic lattice can be subtle, so let us begin with this. In the exercise carried out below, the momentum of the overall 1D lattice will be calculated using classical mechanics. Following this, the analogous quantum mechanical calculation will be carried out.

To lessen confusion over nomenclature, the label $P$ is assigned to the crystal's classical momentum. For a 1D monatomic lattice, $P$ is defined as the mass of a single particle times the sum of the time derivatives of the individual displacements. It is important to distinguish the momentum of the crystal as a whole (the motion *of* its center-of-mass (c.m.) relative to a lab reference frame) from the motions that take place inside the crystal, that is, without changing the crystal's overall momentum relative to a lab reference frame. The analogous situation in gas phase dynamics is the separation of a system into motion *of* a c.m. system and motions that transpire *within* the c.m. system.

In the analogous quantum mechanical case, the normal momentum $\hat{P}_k$ shall be discussed; specifically, its expectation value for the $k^{th}$ normal mode will be calculated. We will see that this also returns a value of zero. In both the classical and quantum cases, we leave aside for the time being $k = 0$.

### Classical Case

With sinusoidal time variation $e^{i\omega_k t}$ or $e^{-i\omega_k t}$ assigned to all displacements associated with the $k^{th}$ normal mode (either exponential can be chosen), the complex displacement at the $n^{th}$ site is given by $A_n = A e^{ikan} e^{\pm i\omega_k t}$, where $A$ is real. Again, keep in mind that all physical quantities are obtained by taking real parts. Differentiation with respect to time results in multiplication by $\pm i\omega_k$. Thus, using the above complex exponentials to express the time behavior, the classical momentum $P$ is given by

$$P = m\sum_n \frac{dA_n}{dt} \tag{2.38}$$

$$= m(\pm i\omega_k)A \underbrace{\left\{\sum_n e^{ikan}\right\}}_{=0} e^{\pm i\omega_k t}. \tag{2.39}$$

Site-to-site phase variation of the displacements is accounted for entirely with the phase factors $e^{ikan}$. We saw previously that the sum inside the bracket in eqn (2.39) vanishes identically. Thus, the step in which the real part of $P$ is taken never arises because $P$ is equal to zero identically. In other words, an individual phonon normal mode (single $k$ value) has no net momentum. It is assumed of course that no external force acts on the crystal to cause it to move as a whole. You might find this surprising because we saw earlier that $k$ is associated with a direction and amount of phase progression.

The overall momentum $P$ is composed of contributions from each of the $n$ sites. It is the site-to-site phase progression that results in the overall momentum being zero. The mathematical statement of this is that $\sum_n e^{ikan} = 0$. What is going on physically is not difficult to visualize, for example, with the diagrams in Chapter 1, Fig. 7 and the transverse displacements in Chapter 1, Fig. 16. For any given $k$ value, half of the momenta point in one direction, while the other half point in the opposite direction. Therefore the net momentum is zero for each $k$ value. The same idea applies to longitudinal compression-rarefaction waves, but these do not make as nice a picture. Thus, as long as $k \neq 0$, there is no overall momentum. Moreover, recall that $k = 0$ is not a vibrational mode. It is overall translation.

## Quantum Case

Let us now return to the relationship between $P$ and $\hat{P}_k$. In the above, $P$ was treated classically, and it was shown that $P = 0$ for a normal mode. This does not mean that the classical momentum $P$ vanishes everywhere. Obviously this cannot be so, or there would be no motion whatsoever, and the system would remain at 0 K. The phase progression $e^{ikan}$ requires that the momentum at any given site is equal and opposite that of a counterpart momentum at another site. In other words, the phases are such that the overall classical momentum for a given phase progression (nonzero $k$ value, which includes all of the sites) vanishes.[7]

Now consider the quantum case. Were we to calculate the quantum mechanical expectation value of $\hat{P}_k$, we would find that it also vanishes. This follows immediately (and without the need to actually carry out a calculation) from the fact that $\hat{P}_k$ acting on the $k^{th}$

[7] Recall the quantum mechanical harmonic oscillator for a single particle. Symmetry requires that the expectation values $\langle x \rangle$ and $\langle p \rangle$ each vanish identically, whereas the quadratic quantities do not vanish: $\langle kx^2/2 \rangle = \langle p^2/2m \rangle = (\omega/2)(v + 1/2)$. Wave packets can be used to describe back and forth oscillation within the well.

mode, $|\, n_k \,\rangle$, raises and lowers it to $|\, n_k + 1 \rangle$ and $|\, n_k - 1 \rangle$, causing the expectation value $\langle n_k \,|\, \hat{P}_k \,|\, n_k \,\rangle$ to vanish. However, $\hat{P}_k$ enters the Hamiltonian quadratically, so there is no problem with the fact that its expectation value vanishes. The expectation value of $\hat{P}_k{}^2$ does not vanish. In mathematical terms, this is seen by writing $\hat{P}_k{}^2 = \hat{P}_k \hat{P}_k$ and inserting closure between the two $\hat{P}_k$'s:

$$\langle n_k \,|\, \hat{P}_k{}^2 \,|\, n_k \,\rangle = \sum_{n_{k'}} \langle n_k \,|\, \hat{P}_k \,|\, n_{k'} \rangle \langle n_{k'} \,|\, \hat{P}_k \,|\, n_k \,\rangle \tag{2.40}$$

$$= K \sum_{n_{k'}} \langle n_k \,|\, \left( \hat{a}_k{}^\dagger - \hat{a}_{-k} \right) |\, n_{k'} \rangle \langle n_{k'} \,|\, \left( \hat{a}_k{}^\dagger - \hat{a}_{-k} \right) |\, n_k \,\rangle \tag{2.41}$$

where $K$ is a constant. This gives the expected result. Details are assigned as an exercise.

When the lattice is not monatomic, the overall momentum still vanishes (classically and quantum mechanically). Of course, we know from common experience that lattice vibrations are transported through a crystalline lattice. Mathematically, wave packets are used to represent phonon waves traveling in any direction, dispersing, and so on. Wave packets are a more intuitive way to think of phonons than trying to imagine how waves having single $k$ values – the normal modes – behave. Nonetheless, if all that takes place is propagation, in a perfectly harmonic crystal, of wave packets that are comprised of different numbers of quanta of the different normal modes, there is no mechanism for crystal momentum to be created or destroyed.

## Anharmonicity

The phonons under consideration are quanta of a Hamiltonian in which the potential energy, which can be expressed in terms of a Taylor series expansion about the equilibrium position, is approximated by just the quadratic term. Obviously this is only a zero-order approximation to any realistic crystal, or for that matter any other related physical system. No potential has ever been found in a solid, liquid, or isolated molecule that contains just the quadratic term and no higher-order terms.

A Taylor series expansion of a given potential energy contains numerous higher-order terms. For a single oscillator, the potential, expanded about its ($x = 0$) equilibrium position, can be expressed as:

$$V(x) = \tfrac{1}{2}\kappa x^2 + ax^3 + bx^4 + cx^5 + \ldots.$$

For an ensemble of different modes, the number of cross terms is large, with level proximities influencing strongly the respective coupling efficiencies. All of these additional terms in a potential fall under the heading of anharmonicity. They are not simply small corrections. They are responsible for many important things. For example, without anharmonicity: (1) a solid would not undergo thermal expansion because $\langle x^2 \rangle$ would remain at its equilibrium value regardless of the degree of vibrational excitation; (2) phonons would have an infinite lifetime; and (3) most importantly for the present discussion, the thermal conductivity of a crystal would be infinite.

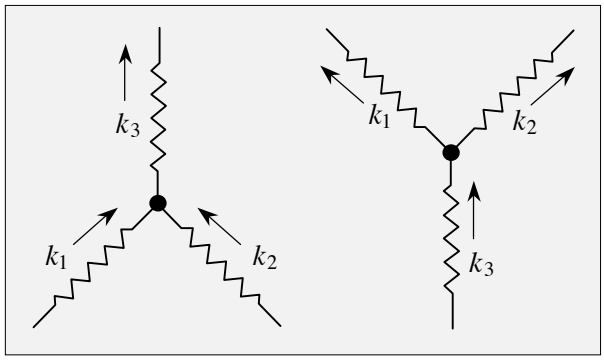


To see why this latter point is so, consider couplings among phonon states. Anharmonic couplings can be expressed in terms of raising and lowering operators, which makes clear their role in coupling modes to one another. As mentioned earlier, the anharmonic terms of most importance are those that couple the modes to one another. For example, suppose one quantum of one mode has energy that is approximately equal to two quanta of another mode and there is a term in the potential that couples these vibrations. This provides a pathway for deactivation and/or excitation transfer that does not exist in a purely harmonic crystal. It can be said that the phonon has a finite lifetime.

## 2.10. Bragg Scattering

Consider a wave incident on a crystal at some angle θ, as indicated in Fig. 11(a). It is assumed that the crystal is rigid. We shall take as our wave an *x*-ray photon with well defined energy. A slow, monoenergetic neutron can also be used. The two incoming rays are assigned equal phases in the plane indicated with a solid red line perpendicular to the rays on the left side. A phase difference accrues in the outgoing rays because the distances traveled by the rays, starting say from the red reference plane on the left, differ by $2a\sin\theta$ when the scattered rays emerge as outgoing rays. In other words, the distance between the two red planes on the right side of Fig. 3.11(a) is $2a\sin\theta$. This is also indicated in Fig. 11(b). Constructive interference occurs when $2a\sin\theta$ is equal to an integral number of *x*-ray wavelengths. This is referred to as the Bragg condition:

$$2a\sin\theta = n\lambda\,. \tag{2.42}$$

Rays are used as a means of registering phase difference. Of course, we are dealing with electromagnetic radiation, which comes in waves, not rays. For example, think of a uniform plane wave with wave vector $\boldsymbol{k}_{in}$ and uniform intensity in the plane whose normal is in the same direction as $\boldsymbol{k}_{in}$. Though it is obviously a wave, we can still use the ray picture to obtain the Bragg condition.

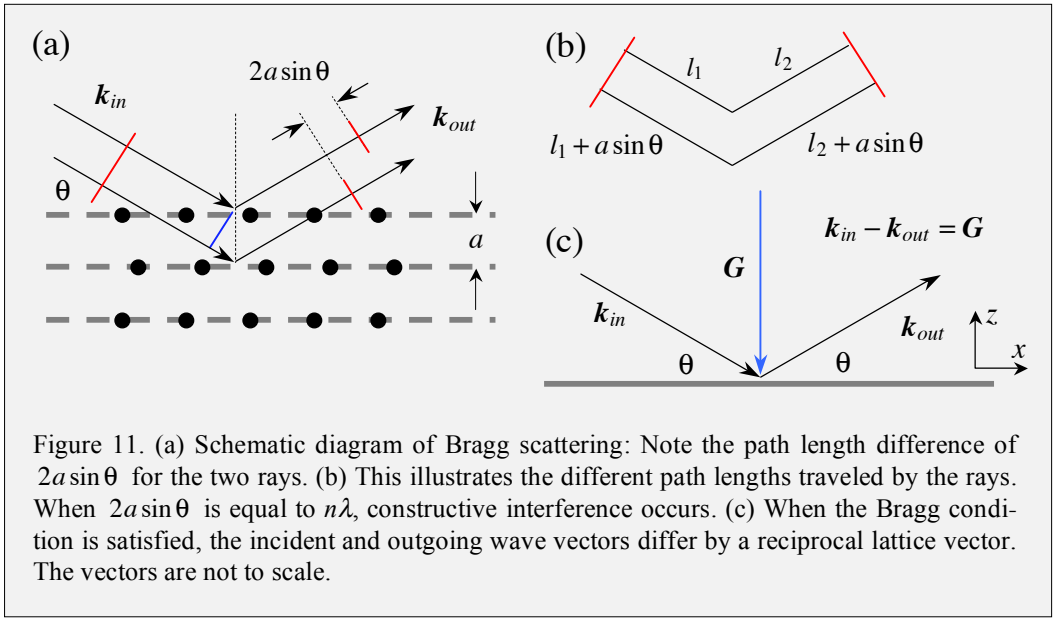


Figure 11. (a) Schematic diagram of Bragg scattering: Note the path length difference of $2a\sin\theta$ for the two rays. (b) This illustrates the different path lengths traveled by the rays. When $2a\sin\theta$ is equal to $n\lambda$, constructive interference occurs. (c) When the Bragg condition is satisfied, the incident and outgoing wave vectors differ by a reciprocal lattice vector. The vectors are not to scale.

Figure 11(c) indicates that when the Bragg condition is satisfied, $\boldsymbol{k}_{in} - \boldsymbol{k}_{out}$ is equal to a reciprocal lattice vector $\boldsymbol{G}$. For example,

$$\boldsymbol{k}_{out} = k_x \hat{x} + k_z \hat{z} = k\cos\theta\,\hat{x} + k\sin\theta\,\hat{z} \tag{2.43}$$

$$\boldsymbol{k}_{in} = k\cos\theta\,\hat{x} - k\sin\theta\,\hat{z}\,. \tag{2.44}$$

Therefore,

$$\boldsymbol{k}_{in} - \boldsymbol{k}_{out} = -2k\sin\theta\,\hat{z} \tag{2.45}$$

$$= -2\frac{2\pi}{\lambda}\sin\theta\,\hat{z} \tag{2.46}$$

$$= -2\pi\frac{2\sin\theta}{\lambda}\hat{z}\,. \tag{2.47}$$

Using the Bragg condition given by eqn (2.42) to identify the angles at which the maximum scattering intensities occur ( $2a\sin\theta = n\lambda$ ), this becomes

$$\boldsymbol{k}_{in} - \boldsymbol{k}_{out} = -\frac{2\pi}{a}n\,\hat{z} \tag{2.48}$$

$$= \boldsymbol{G}. \tag{2.49}$$

The minus sign on the right hand side of eqn (2.48) is in accord with the direction of $\boldsymbol{G}$ and the definition of the $x$ and $z$ directions indicated in Fig. 11(c). You can see visually that the larger the angle $\theta$, the larger the reciprocal lattice vector $\boldsymbol{G}$, and the larger the value of $n$ in eqn (2.48).

Many lattice sites are involved, so a momentum change of $\hbar\boldsymbol{G}$ does not affect noticeably the movement of the lattice, and scattering can be taken to be elastic. Maxima in the scattered signal appear at $\theta$ values that satisfy the Bragg condition given by eqn (2.42). These directions ($\theta$ values) follow the rule that the difference in incident and scattered wave vectors is a reciprocal lattice vector:

$$\boxed{\boldsymbol{k}_{in} - \boldsymbol{k}_{out} = \boldsymbol{G}} \tag{2.50}$$

where $|\boldsymbol{G}| = (2\pi/a)n$ . This admittedly rough description does an adequate job of describing $x$-ray and slow neutron diffraction / interference patterns.

## 2.11. A Phonon is Created

Next, consider a scattering process in which a phonon is created, as indicated in Fig. 12(a). This differs from the case presented above, where the lattice was taken as rigid. The incident and scattered wave vectors might differ by an amount that is too large for the phonon to be accommodated in the first Brillouin zone. However, we know that all phonon wave vectors must lie within the first Brillouin zone, and that a phonon wave vector that, at first sight, appears to lie outside the first Brillouin zone is equivalent to one that lies in the first Brillouin zone. The latter is obtained by compensating with whatever reciprocal lattice vector is required to get the phonon into the first Brillouin zone. In other words, the phonon wave vector, $\boldsymbol{k}$, must satisfy the relation

$$\boldsymbol{k}_{in} = \boldsymbol{k}_{out} + \boldsymbol{k}_{phonon} + \boldsymbol{G} \,. \tag{2.51}$$

Again, it is understood that $\boldsymbol{k}_{phonon}$ lies in the first Brillouin zone, and $\boldsymbol{G}$ is whatever reciprocal lattice vector is required to ensure that $\boldsymbol{k}$ lies in the first Brillouin zone. Keep in mind that eqn (2.51) refers to Fig. 12(a) rather than Fig. 11.

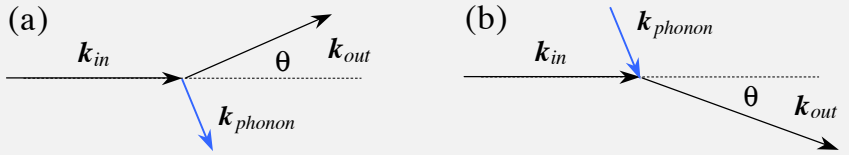


Figure 12. The phonon wave vector either (a) subtracts from, or (b) adds to the incident wave vector ( $\boldsymbol{k}_{in}$ ) to yield the outgoing wave vector ( $\boldsymbol{k}_{out}$ ), depending on whether the phonon is created or annihilated, respectively. Namely, in (a) a phonon is created, while in (b) a phonon is annihilated. Keep in mind that the phonon wave vector might need to be augmented by a reciprocal lattice vector to keep the phonon wave vector in the first Brillouin zone.

At the same time, conservation of momentum tells us that perhaps it is unwise to ignore the reciprocal lattice vectors $\boldsymbol{G}$ as if they did not exist, even though they have no bearing on the resulting phonon. What happens is that the crystal acquires the momentum associated with $\boldsymbol{G}$. However, because the crystal is heavy, the amount of energy imparted to it is minuscule. The smallness of the imparted energy is dramatic. The translational energy acquired by the crystal is far too small to worry about. Go ahead and make an estimate of $(\hbar G)^2/2m$ – you will see that it is tiny. In many books, you will find eqn (2.51) written with each term multiplied by $\hbar$. This is likely to be confusing when you first encounter it. With $\hbar$ multiplying all the terms, eqn (2.51) takes on the appearance of a momentum conservation equation. However, because $\hbar\boldsymbol{k}$ is not a true momentum, eqn (2.51) is a statement of *wave vector conservation* or *crystal momentum conservation*.

## 2.12. Phonon-Phonon Scattering

The above considerations set the stage for a discussion of crystal momentum relaxation in a crystal. The idea is this. Unless phonons interact with one another (or with electrons, defects, surfaces, etc.) there can be no dissipation of their crystal momentum, and consequently the thermal conductivity is infinite. In other words, phonons pass freely throughout the crystal. Suppose two phonons, $\boldsymbol{k}_1$ and $\boldsymbol{k}_2$, interact and are annihilated thereby creating a third phonon, $\boldsymbol{k}_3$. If the $\boldsymbol{k}_1$ and $\boldsymbol{k}_2$ phonons lie well within the first Brillouin zone, so does the $\boldsymbol{k}_3$ phonon. Figure 13(a) shows how this works. This situation prevails at low temperatures because the phonons have low energy. They occupy mainly the low-$k$ region of the acoustic branches.

Now consider higher temperatures, such that phonons are present all the way to the Brillouin zone edges of the acoustic branches. Suppose two energetic phonons are annihilated to create a third phonon, but the resultant $\boldsymbol{k}_1 + \boldsymbol{k}_2$ lies outside the first Brillouin zone. A phonon cannot be created with this wave vector because phonons do not exist outside the first Brillouin zone. The phonon that is created differs from $\boldsymbol{k}_1 + \boldsymbol{k}_2$ by a reciprocal lattice vector $\boldsymbol{G}$ such that $\boldsymbol{k}_1 + \boldsymbol{k}_2 + \boldsymbol{G} = \boldsymbol{k}_3$, where $\boldsymbol{k}_3$ lies within the first Brillouin zone, as depicted in Fig. 13(b). This is called an umklapp process (German *umklappen*: to turn over) whereas the situation in Fig. 13(a), where the phonons lie within the Brillouin zone, is referred to as a normal process.

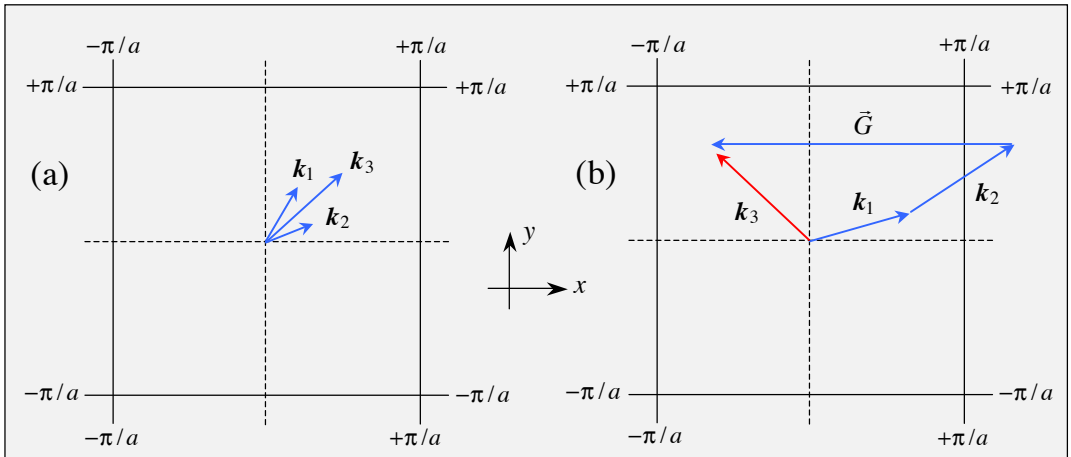


Figure 13. (a) The resultant wave vector lies within the first Brillouin zone. This is a *normal* process. (b) The resultant wave vector lies outside the first Brillouin zone. A reciprocal lattice vector returns the wave vector to the first Brillouin zone. This is an *umklapp* process.

In Fig. 13(b), a simple process is indicated in which $\boldsymbol{G}$ lies along one of the crystal axes. For a 3D crystal, $\boldsymbol{G}$ can be made of components in different directions. For example, suppose $\boldsymbol{k}_1$ and $\boldsymbol{k}_2$ each extend from the origin to near the $+\pi/a, +\pi/a$ corner on the upper right. In this case, a reciprocal lattice vector $\boldsymbol{G} = -(2\pi/a)\hat{x} - (2\pi/a)\hat{y}$ is required to return the system to the first Brillouin zone. Regardless of such details, the important fact is that this umklapp process can dissipate crystal momentum.

## 2.13. High-Temperature Limit

At high temperatures and with a good quality crystal, umklapp processes dominate crystal momentum relaxation. In this regime, the thermal conductivity $\kappa = Cvl/3$ is proportional to the scattering length $l$. The heat capacity $C$ is independent of temperature ($C = 3nk_B$), and the speed of sound depends weakly on temperature. The scattering length depends on the phonon density. This is analogous to gas phase kinetics, where the mean distance between collisions varies inversely with number density.

The phonon density depends linearly on temperature, as can be seen by noting the high temperature limit:

$$\langle n_k \rangle = \frac{1}{e^{\omega_k / k_B T} - 1} \quad \Rightarrow \quad k_B T / \omega_k \,. \tag{2.52}$$

Thus, we find that $l$ varies at least as strongly as $T^{-1}$. The variation can be stronger, depending on multiphonon processes, which are nontrivial to model. In experiments, the thermal conductivity is found to vary as $T^{-z}$, where $1 \le z \le 2$.

## 2.14. Low-Temperature Limit

At low temperatures, phonon collisions are dominated by normal processes, which conserve crystal momentum, as indicated in Fig. 13(a). One can say that the umklapp processes are frozen out. This has the interesting consequence that at sufficiently low temperatures there is no mechanism for the thermalization of phonons. In other words, heat can flow freely in the absence of a temperature gradient. Thus, the thermal conductivity of a perfect electrical insulator crystal is infinite in the low temperature limit. Of course we know that this is not the case. As the low temperature limit is approached, the number of phonons that can participate in umklapp processes falls off rapidly with temperature. The phonons that do participate are energetic ($\omega_k \sim k_B \Theta_D$), so the average number of these phonons is

$$\langle n_k \rangle \quad \Rightarrow \quad \frac{1}{e^{\Theta_D / T} - 1} \sim e^{-\Theta_D / T} \tag{2.53}$$

Because the number of effective collisions falls off exponentially as $e^{-\Theta_D / T}$, the mean scattering length (or the mean time between effective phonon collisions) varies as $e^{\Theta_D / T}$ or something close to it, say $e^{T_0 / T}$. As a consequence, defects, impurities, isotopes, and even sample size limit the thermal conductivity. This is illustrated in Fig. 14.

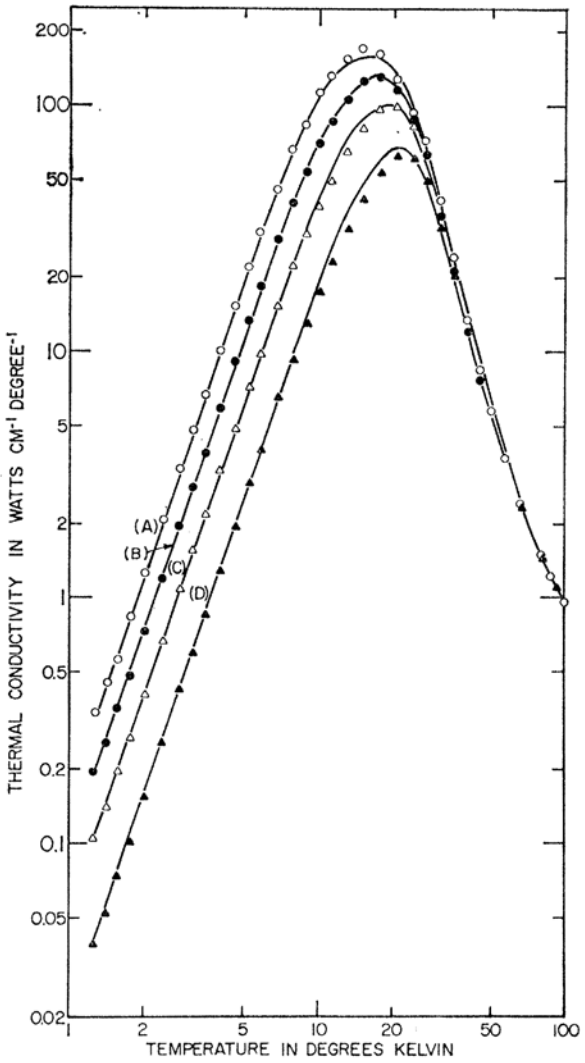


Figure 14. Thermal conductivity $\kappa$ (in units of $\mathrm{W \cdot cm^{-1} \cdot K^{-1}}$) versus temperature for isotopically pure LiF crystals of different size: Below 10 K, $\kappa$ varies as $T^3$. This variation is due to the temperature dependence of the heat capacity in the low temperature regime. Curves (A) – (D) are for crystals having different dimensions (in mm): (A) 7.55 × 6.97; (B) 4.24 × 3.77; (C) 2.17 × 2.10; and (D) 1.23 × 0.91. These crystals are sufficiently free of defects and impurities that these imperfections do not contribute to the thermal conductivity, even at the lowest temperatures. For temperatures below ~ 10 K, the scattering length $l$ is of the order of the size of the crystal. Taken from P. D. Thatcher, Phys. Rev. **156**, 975 (1967).

Identity theft